Preprints of the 18th IFAC World Congress
Milano (Italy) August 28 - September 2, 2011

Nanopositioning with multiple sensors: MISO control and inherent sensor fusion

Abu Sebastian and Angeliki Pantazi

IBM Research - Zurich, Rüschlikon, CH-8803 Switzerland
(ase@zurich.ibm.com,agp@zurich.ibm.com)

Abstract: There is a strong motivation for using multiple sensors for feedback control in ultra-high accuracy data storage devices such as a probe-based data storage device. One elegant way to design such controllers using multiple sensors is to design a direct multi-input-single-output (MISO) controller using either the $\mathcal{H}_2$ or $\mathcal{H}_\infty$ control design paradigm. In this paper we discuss the control of a micro-scanner used in a probe-based data storage device. Two sensors, a global position sensor and medium derived positional information, are employed simultaneously. MISO controllers are designed to obtain the desired frequency separation in closed loop performance. These controllers are investigated in detail to understand their underlying structure and the inherent sensor fusion that takes place during the control. Comparisons are made with conventional Kalman filtering and $\mathcal{H}_\infty$ filtering problems.
Keywords: Nanopositioning, $\mathcal{H}_2$ control, $\mathcal{H}_\infty$ control, sensor fusion

1. INTRODUCTION

Probe-based data storage has been a subject of intensive research due to its potential for achieving ultra-high storage densities in excess of 1 Tbit/in^2. Several approaches to probe storage have been studied, including thermo-mechanical recording on polymer films, electrical recording in ferroelectric media and the electrical recording of crystalline/amorphous marks in phase-change materials (Pantazi et al. (2008); Forrester et al. (2009); Jo et al. (2009)). Of these, thermo-mechanical storage using polymer media is the most advanced. A data-storage device prototype based on this concept was presented in Pantazi et al. (2008). It consisted of an array of cantilevers recording information on a thin polymer film which was spun coat onto the scan table of a micro-scanner. The polymer media is moved relative to the cantilever array during the operation of the device. Both the cantilever array and the micro-scanner were micro-fabricated. The error-free recording and reading back of data at the ultrahigh areal density of 840 Gb/in^2 was demonstrated using this prototype.

One of the key challenges associated with data storage at such areal density is nanopositioning. Positioning accuracies of less than a nanometer is essential to achieve the desired error rate (Pantazi et al. (2007); Sebastian et al. (2008b)). Moreover, unlike regular scanning probe applications that require comparable positioning accuracies (Salapaka and Salapaka (2008)), in data storage applications we require absolute positioning as opposed to relative positioning. It is essential to reliably reach a target data track over extended periods of time. Moreover, the requirement on disturbance rejection is more stringent in a data storage device. Feedback control based on multiple sensors was found to be essential to tackle these challenges (Pantazi et al. (2007)). The use of multiple sensors have also been shown to be advantageous for the control of piezo-electric tube actuators (Fleming et al. (2008); Mahmood et al. (2009)).

There are multiple ways to approach the nanopositioning problem with multiple sensors. It is possible to have switching controllers that operate on one sensor during a certain period of time and then switches to an alternate sensor during another period of time. This strategy is typically employed when the two sensors have distinctly different noise characteristics and when the better sensor information is not available during certain periods of time. An alternate approach is to perform sensor fusion with the multiple sensors and then employ a feedback controller based on the fused sensor information. Kalman filtering, $\mathcal{H}_2$ filtering and $\mathcal{H}_\infty$ filtering are all candidates for sensor fusion. However, the lack of guaranteed stability or stability margins is a significant drawback of this approach.

Yet another approach is to design a multi-input-single-output (MISO) controller K that utilizes the multiple sensor information and outputs the control signal. This rather elegant, direct control approach was first presented in Pantazi et al. (2005) where an $\mathcal{H}_\infty$ control design was performed. In this paper we present a detailed study of the multi-sensor based nanopositioning problem as applied to the probe-based data storage device prototype. The MISO controller design problem is formulated based on the noise characteristics of the sensors and the specifications for disturbance rejection. Both $\mathcal{H}_2$ and $\mathcal{H}_\infty$ controllers are designed. The primary objective is to understand the structure of controllers that arise out of the direct control approach. Both $\mathcal{H}_\infty$ and $\mathcal{H}_2$ controllers lend themselves to possible separation structures with an estimator and a regulator. In which case it would be of interest to relate the underlying estimator with traditional sensor fusion approaches. Transfer functions showing the closed loop performance and the inherent sensor fusion are presented. Simulations are performed to illustrate the efficacy of the MISO controller and the inherent sensor fusion.

2. SYSTEM DESCRIPTION

In the probe-based data storage device prototype, a MEMS-based micro-scanner with two-dimensional motion capability (Lantz et al. (2007)) is used to position the storage medium relative to the array of read/write probes. During the regular operation of the device, a scan operation is performed along the fast X-scan direction while stepping in the Y-scan direction. Global thermal position sensors (TPS) are used to sense the scanner motion

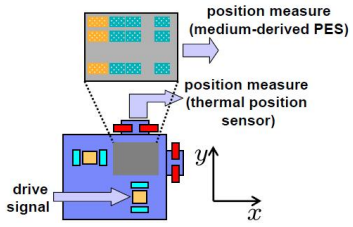

Fig. 1. Schematic illustrating the MEMS microscanner, the global thermal position sensor and medium derived PES.

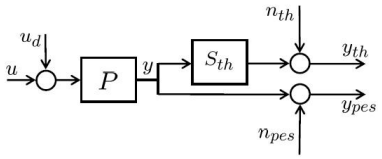

Fig. 2. Block diagram representation of the scanner and sensors

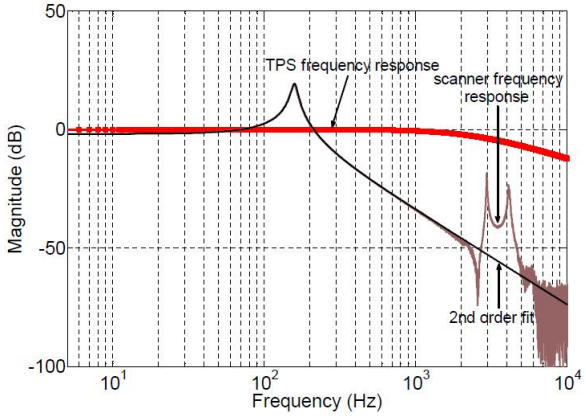

Fig. 3. (a) The scanner dynamics along the Y-scan direction (b) The spectral characteristics of the thermal position sensor noise and PES noise

along both scan directions (Lantz et al. (2005)). These sensors can provide position information across the whole travel range of the scanner. However, they suffer from low frequency noise and drift. This is particularly detrimental for positioning along the Y-scan direction as low frequency noise will result in deviations from the desired track thus resulting in reduced signal-to-noise ratio. Hence in addition to the global position sensors we also employ the medium derived position error signal (PES). This is positional information derived from pre-written servo patterns written in dedicated servo fields with ultra-high precision (Sebastian et al. (2008a)). Clearly PES does not have low frequency noise characteristics. In fact PES noise is rather white in nature and mostly governed by media roughness and electronic noise (Sebastian et al. (2007); Pozidis et al. (2010)). Moreover, PES has a limited range. The microscanner and the sensors are schematically depicted in Figure 1.

A block diagram representation is shown in Figure 2. The scanner dynamics along the Y-scan direction is captured by P. The TPS exhibits first order dynamics and is modelled by S_{th} (Sebastian and Wiesmann (2008)). y denotes the position of the scanner along the Y-scan direction and y_{th} and y_{pes} denote the measured position using the TPS and PES respectively. n_{th} and n_{pes} denote the TPS and PES noise respectively. The scanner dynamics along the Y-scan direction is well captured by a second order model as shown in Figure 3(a). The experimentally obtained spectral characteristics of n_{th} and n_{pes} are shown in Figure 3(b). It can be seen that n_{th} has a strong 1/f characteristic. On the other hand beyond a certain frequency n_{th} is better than n_{pes}. The input disturbance is captured by u_d. During the scan operation, the primary requirement for the Y-scan direction is to maintain a constant position while scanning along the X-scan direction in the presence of various disturbances. In a mobile storage device the input disturbances that need to be rejected typically have a frequency content less than 500 Hz. However in the device prototype this requirement is slightly relaxed. There is also some cross-coupling between the scan axes which can be treated as disturbance. The spectral characteristics of the measurement noise and the requirement on disturbance rejection have to be taken into account during the control design.

3. FORMULATION OF THE CONTROL PROBLEM

The control problem is to regulate the scanner position in the presence of input disturbance and the measurement noise from the two sensors. The control problem is formulated based on the scanner and sensor dynamics, noise characteristics of the sensors and the requirements on disturbance rejection. As mentioned earlier, the approach taken is to use both the sensors simultaneously using a MISO control design. It is expected that the necessary "frequency separation" in terms of sensor allocation will be addressed by this controller.

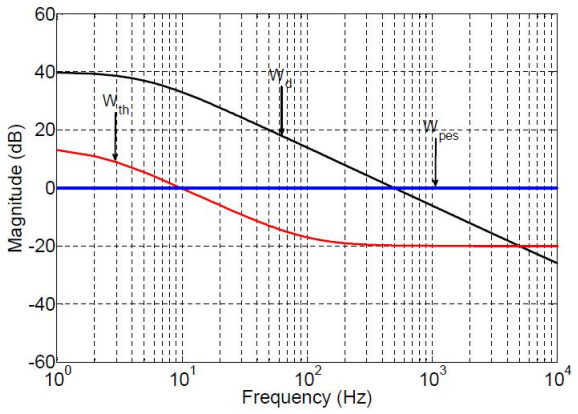

Fig. 4. The frequency response of the filters W_d, W_{th} and W_{pes}

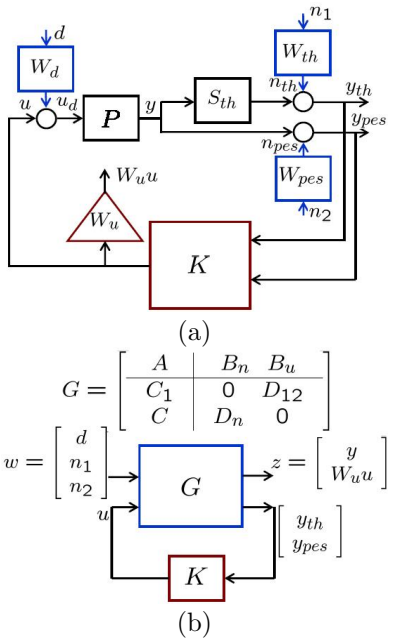

Fig. 5. (a) Block diagram representation of the scanner, sensors, augmented filters and the two input single output controller. (b) LFT formulation of the control design problem.

The filters W_d, W_{th} and W_{pes} are introduced during the control design process to capture the spectral characteristics of u_d, n_{th} and n_{pes} respectively. W_{th} and W_d are chosen to be first order filters whereas W_{pes} is just a gain. The magnitude response of these filters are shown in Figure 4. The inputs to the filters W_d, W_{th} and W_{pes} are white noise signals d, n_1 and n_2 which are uncorrelated. A block diagram representation of the system and the controller is shown in Figure 5(a). To ensure a bounded control signal an additional constant weighting factor W_u is introduced. The state space equations governing the dynamics of the scanner and sensors along with the augmented filters is given by

$$\overbrace{\begin{bmatrix} \dot{x}_{p_1} \\ \dot{x}_{p_2} \\ \dot{x}_d \\ \dot{x}_s \\ \dot{x}_{th} \end{bmatrix}}^{\dot{\mathbf{x}}} = \overbrace{\begin{bmatrix} A_{p11} & A_{p12} & B_{p11}C_d & 0 & 0 \\ A_{p21} & A_{p22} & B_{p21}C_d & 0 & 0 \\ 0 & 0 & A_d & 0 & 0 \\ BsC_{p11} & BsC_{p12} & 0 & A_s & 0 \\ 0 & 0 & 0 & 0 & A_{th} \end{bmatrix}}^{A} \overbrace{\begin{bmatrix} x_{p_1} \\ x_{p_2} \\ x_d \\ x_s \\ x_{th} \end{bmatrix}}^{\mathbf{x}} + \overbrace{\begin{bmatrix} B_{p11} \\ B_{p21} \\ 0 \\ 0 \\ 0 \end{bmatrix}}^{B_u} u + \overbrace{\begin{bmatrix} B_{p11}D_d & 0 & 0 \\ B_{p21}D_d & 0 & 0 \\ B_d & 0 & 0 \\ 0 & 0 & 0 \\ 0 & B_{th} & 0 \end{bmatrix}}^{B_n} \begin{bmatrix} d \\ n_1 \\ n_2 \end{bmatrix} \quad (1)$$

$$\begin{bmatrix} y_{th} \\ y_{pes} \end{bmatrix} = \overbrace{\begin{bmatrix} 0 & 0 & 0 & C_s & C_{th} \\ C_{p11} & C_{p12} & 0 & 0 & 0 \end{bmatrix}}^{C} \overbrace{\begin{bmatrix} x_{p_1} \\ x_{p_2} \\ x_d \\ x_s \\ x_{th} \end{bmatrix}}^{\mathbf{x}} + \overbrace{\begin{bmatrix} 0 & D_{th} & 0 \\ 0 & 0 & D_{pes} \end{bmatrix}}^{D_n} \begin{bmatrix} d \\ n_1 \\ n_2 \end{bmatrix}$$

$\left[\begin{array}{c|c} A_p & B_p \\ \hline C_p & 0 \end{array}\right]$, $\left[\begin{array}{c|c} A_s & B_s \\ \hline C_s & 0 \end{array}\right]$, $\left[\begin{array}{c|c} A_d & B_d \\ \hline C_d & D_d \end{array}\right]$ and $\left[\begin{array}{c|c} A_{th} & B_{th} \\ \hline C_{th} & D_{th} \end{array}\right]$ denote the state space descriptions of P, S, W_d and W_{th} respectively. D_{pes} is a constant gain equal to W_{pes}.

An LFT formulation of the control design problem is presented in Figure 5(b) where , $C_1 = \begin{bmatrix} 1 & 0 & 0 & 0 & 0 \\ 0 & 0 & 0 & 0 & 0 \end{bmatrix}$ and $D_{12} = \begin{bmatrix} 0 \\ W_u \end{bmatrix}$. The objective of the control problem is to design a stabilizing controller K such that it minimizes or bounds a certain norm of the closed loop transfer function $T_{zw} = F_l(G, K)$.

4. TWO SENSOR BASED $\mathcal{H}_2$ CONTROL

First we consider the $\mathcal{H}_2$ control design using the two sensor signals y_{pes} and y_{th}. With respect to Figure 5(b), the optimization problem being solved is

$$K^2_{con} = \min_K \|T_{zw}\|_2 \quad (2)$$

The objective is to understand the structure of the controller. The $\mathcal{H}_2$ problem is solved such that the resulting controller retains the separation structure with an estimator and a state feedback controller. The state variables are also retained during the entire solution process.

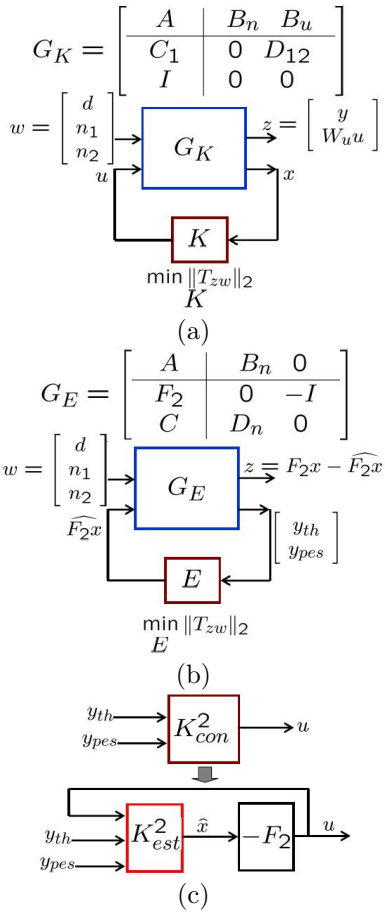

Fig. 6. $\mathcal{H}_2$ solution: (a) LFT formulation of the full state information control problem (b) LFT formulation of the associated $\mathcal{H}_2$ filtering problem. (c) Schematic illustrating the separation structure in the MISO $\mathcal{H}_2$ controller.

It can be shown that the state feedback controller F_2 is the solution to the full state information problem as formulated in Figure 6(a) (Doyle et al. (1989)). The objective is to find the controller that minimizes $\|T_{zw}\|_2$ given that the state information of G_K is available. It can be shown that F_2 is equivalent to the linear quadratic regulator problem associated with the system described by

$$\dot{\mathbf{x}} = A\mathbf{x} + B_u u \tag{3}$$
$$y = \begin{bmatrix} 1 & 0 & 0 & 0 & 0 \end{bmatrix} \mathbf{x}.$$

minimizing the objective function

$$J_c = \int_0^\infty \left(y(t)^2 + W_u^2 u(t)^2 \right) dt. \tag{4}$$

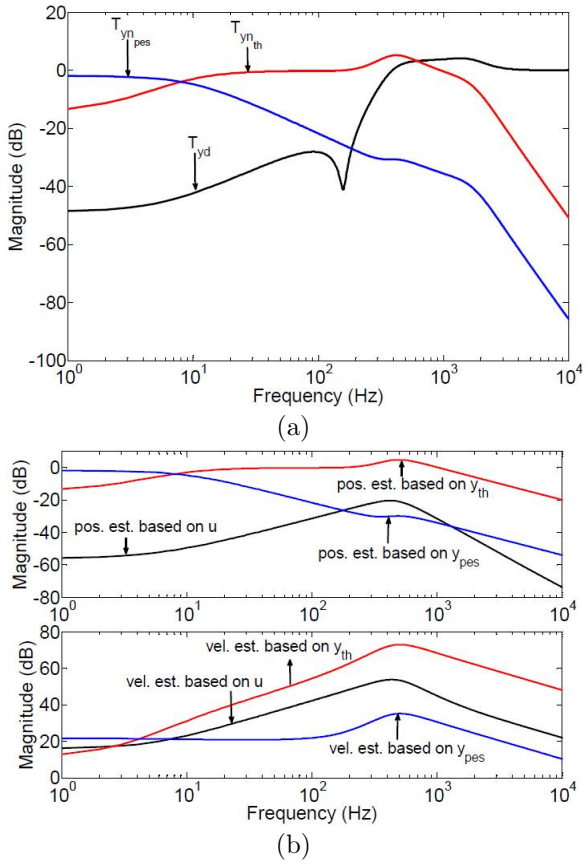

Fig. 7. (a) The closed-loop transfer functions associated with direct $\mathcal{H}_2$ control. (b) The inherent sensor fusion occurring during direct $\mathcal{H}_2$ control.

The estimation problem associated with the $\mathcal{H}_2$ control problem is to find the observer that provides the best estimate of $F_2 x$ as formulated in Figure 6(b). However the best estimate of $F_2 x$ in the two norm sense is the best estimate of x weighted by F_2. Hence the estimation problem is identical to the optimal state estimation problem in the two norm sense. Let the optimal observer gain be given by L_2. Then the state estimator (K_{est}^2) dynamics are described by

$$\dot{\hat{\mathbf{x}}} = A\hat{\mathbf{x}} + B_u u + L_2 \left(\begin{bmatrix} y_{th} \\ y_{pes} \end{bmatrix} - C\hat{\mathbf{x}} \right). \tag{5}$$

This particular state estimation problem is identical to a Kalman filtering problem associated with the state space equations

$$\dot{\mathbf{x}} = A\mathbf{x} + B_u u + B_n n_p \tag{6}$$
$$\begin{bmatrix} y_{th} \\ y_{pes} \end{bmatrix} = C\mathbf{x} + n_m.$$

In this formulation the process noise $n_p = \begin{bmatrix} d & n_1 & n_2 \end{bmatrix}^T$ while the measurement noise $n_m = \begin{bmatrix} D_{th} n_1 \\ D_{pes} n_2 \end{bmatrix}$. The process noise and measurement noise are correlated with the covariance matrices given by $E(n_p n_p^T) = I$, $E(n_m n_m^T) = \begin{bmatrix} D_{th}^2 & 0 \\ 0 & D_{pes}^2 \end{bmatrix}$ and $E(n_p n_m^T) = \begin{bmatrix} 0 & 0 \\ D_{th} & 0 \\ 0 & D_{pes} \end{bmatrix}$. The Kalman filter gain in this case is identical to L_2 obtained from the estimation problem associated with the MISO $\mathcal{H}_2$ control problem.

To summarize, the estimator and regulator associated with direct MISO $\mathcal{H}_2$ control is presented in Figure 6(c). The controller consists of:

- A state feedback controller obtained from full state information $\mathcal{H}_2$ control or as a solution to an LQR problem corresponding to the objective function given by (4)
- An optimal state estimator in the 2-norm sense using both the sensors. The estimation problem is identical to a Kalman filtering problem.

The closed loop transfer functions corresponding to direct $\mathcal{H}_2$ control are presented in Figure 7(a). These transfer functions relate the scanner position y to d, n_{th} and n_{pes}. The disturbance rejection bandwidth is 341 Hz. The frequency separation is clearly visible from the transfer functions $T_{yn_{th}}$ and $T_{yn_{pes}}$ where the PES is the dominant sensor at low frequencies up to 8Hz. The estimator within the direct $\mathcal{H}_2$ controller also results in an inherent sensor fusion. This sensor fusion is captured by the transfer functions presented in Figure 7(b). The estimation of two of the state variables, position and velocity of the scanner, is illustrated.

5. TWO SENSOR BASED $\mathcal{H}_\infty$ CONTROL

In this section the MISO $\mathcal{H}_\infty$ controller is analyzed. The control problem is formulated in Figure 5(b) where the objective is to find a stabilizing controller K such that $\|T_{zw}\|_\infty < \gamma$. For the $\mathcal{H}_\infty$ control problem it was found that for a $\gamma_f = 1.0039$, there exists a stabilizing controller, K_{con}^∞, such that $\|T_{zw}\|_\infty < \gamma_f$.

To understand the underlying structure of the MISO $\mathcal{H}_\infty$ controller and the inherent sensor fusion, the $\mathcal{H}_\infty$ control problem was solved taking the same approach as in the case of the $\mathcal{H}_2$ control problem and as described in Doyle et al. (1989). As in the previous case the state variables are retained throughout the solution process. To satisfy some of the assumptions required for standard $\mathcal{H}_\infty$ solution it is necessary to scale the input and output signals as described in Zhou et al. (1996). The first step in the solution process is the full state information problem which is presented in Figure 8(a). The objective is to identify the controller that satisfies the condition given in Figure 8(a) with the knowledge of full state information. It can be shown that the central controller is again a state feedback controller with the gain vector denoted by F_∞. Moreover we also obtain a worst case input $w_{worst} = K_w \mathbf{x}$ associated with the full state information problem.

The second step in the solution process is the estimation problem presented in Figure 8(b). It can be seen that this estimator is significantly different from the estimation problem associated with the direct $\mathcal{H}_2$ control problem or even a regular full state $\mathcal{H}_\infty$ filtering problem. Here, the states are scaled by the gain vector $W_u F_\infty$. The modification of the A matrix to $A + B_n K_w$ captures the property that the estimation is performed in the presence of the worst case input for the full information problem. The weighting of the states play a key role in the design

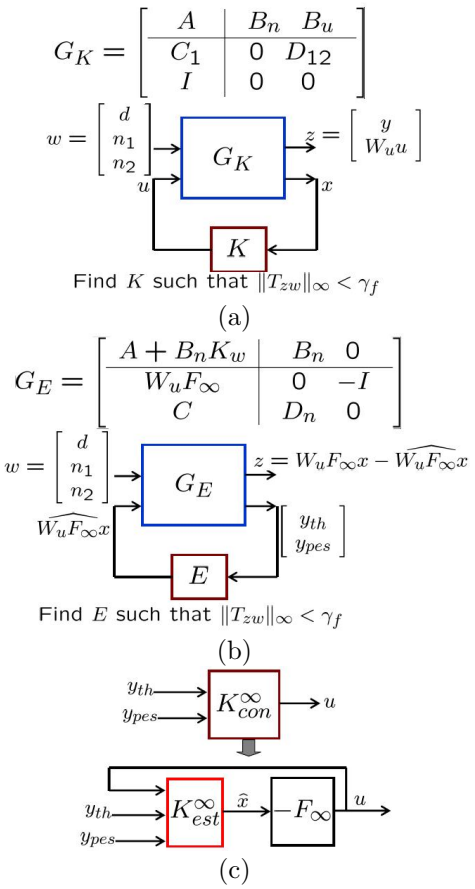

Fig. 8. $\mathcal{H}_\infty$ solution: (a) LFT formulation of the full state information control problem (b) LFT formulation of the associated $\mathcal{H}_\infty$ filtering problem. (c) Schematic illustrating the separation structure in the MISO $\mathcal{H}_\infty$ controller.

of an $\mathcal{H}_\infty$ filter and it is truly remarkable that there is a natural weighting of the states occurring in this estimator problem formulation. There is a preferential estimate of the states weighted by their importance for full state information feedback control. Note that in the case of direct $\mathcal{H}_2$ control, the state estimation problem is disjoint from the control design problem where one could design a Kalman filter and then an LQR feedback controller based on the estimated states.

The state estimator (K^∞_{est}) dynamics corresponding to the $\mathcal{H}_\infty$ controller are described by

$$\dot{\hat{\mathbf{x}}} = (A + B_n K_w)\hat{\mathbf{x}} + B_u u + L_\infty \left(\begin{bmatrix} y_{th} \\ y_{pes} \end{bmatrix} - C\hat{\mathbf{x}} \right), \qquad (7)$$

where L_∞ denotes the filter gain.

A schematic illustration of the separation structure in the direct MISO $\mathcal{H}_\infty$ controller is presented in Figure 8(c). The controller consists of:

- A state feedback controller obtained as a solution to the full state information $\mathcal{H}_\infty$ control problem
- A weighted state estimator which is obtained as a solution to an $\mathcal{H}_\infty$ filtering problem where the states are weighted by the state feedback gain vector and the estimation is done in the presence of the worst case input for the full information problem.

The closed loop transfer functions corresponding to direct $\mathcal{H}_\infty$ control are presented in Figure 9(a). The disturbance

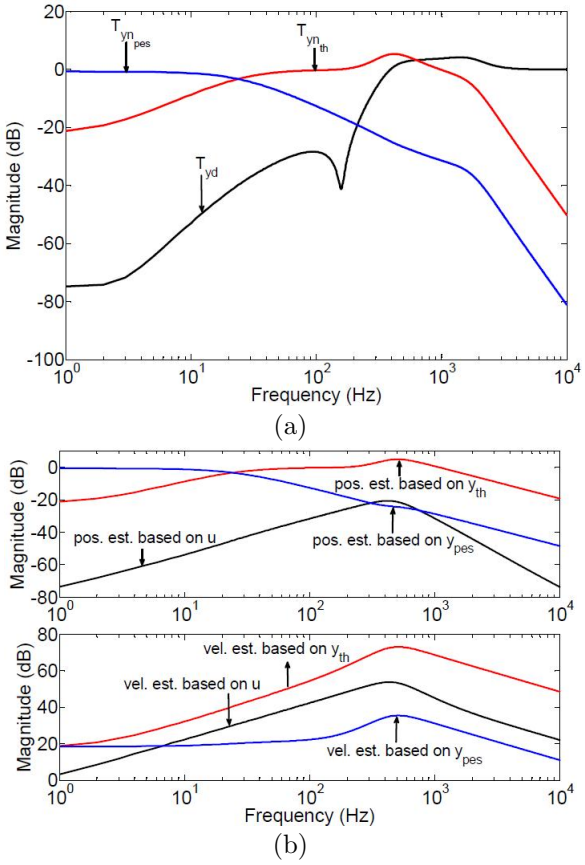

Fig. 9. (a) The closed-loop transfer functions associated with direct $\mathcal{H}_\infty$ control. (b) The inherent sensor fusion occurring during direct $\mathcal{H}_\infty$ control.

rejection bandwidth is almost equal to that of the $\mathcal{H}_2$ controller. However, the extent of disturbance rejection is much better at low frequencies. The frequency separation is again nicely captured with the PES being the dominant sensor at low frequencies below 24 Hz. Even though the estimator within the direct $\mathcal{H}_\infty$ controller is not a conventional state estimator, there is an inherent sensor fusion occurring within the controller as captured by the transfer functions presented in Figure 9(b).

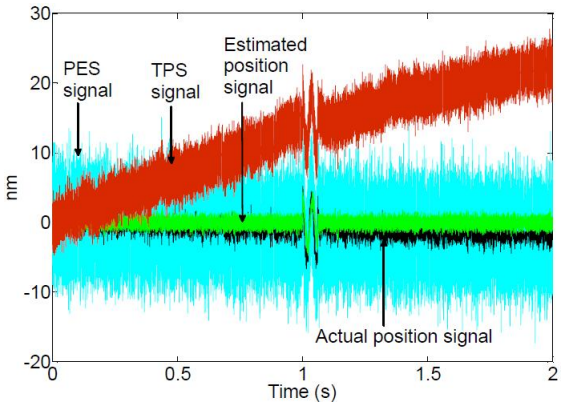

Fig. 10. Simulation results illustrating the functioning of the MISO $\mathcal{H}_\infty$ controller and the inherent estimator.

In Figure 10, simulation results are presented that illustrate the functioning of the $\mathcal{H}_\infty$ controller and the inherent estimator. The objective is to maintain the Y scanner position at zero. The TPS signal and PES signal

are simulated using experimentally obtained models. An additional drift is added to the TPS signal. Also introduced is a signal that simulates a shock signal appearing at the time instant when time equals 1 s. This disturbance signal could have resulted in a scanner motion in excess of 400 nm in the absence of feedback control. The scanner position signal shows that it is not influenced by the drift in the TPS signal and effectively rejects the disturbance signal. The standard deviation of the position signal is 0.8 nm in the absence of external disturbance which is significantly less that the resolution of both the TPS and PES. Also shown is the estimate of the position signal as provided by the inherent estimator within the MISO $\mathcal{H}_\infty$ controller. This estimate is very close to the actual position signal illustrating the quality of the sensor fusion occurring within the MISO controller. This sensor fusion has several advantages. In data storage devices this signal can be used to reliably detect shocks and vibrations. In this case the inherent estimator within the $\mathcal{H}_\infty$ control serves as a disturbance observer. Other applications include realtime identification of scanner cross-coupling and possible drift correction in the case of the TPS.

6. CONCLUSION

The use of multiple sensors for nanopositioning is well motivated in the case of probe-based data storage devices. In one such storage device prototype, a MEMS micro-scanner is used to position the storage medium relative to an array of probes. Thermal position sensors are used to provide positional information of the scanner across the whole travel range. However these global position sensors are susceptible to low frequency noise and drift. Hence, to achieve absolute nanoscale positioning accuracy, it is essential to utilize medium derived position information known as PES. Given the limited range of PES, it is advantageous to employ the global position sensors in addition to it. In this paper we discuss the control of the micro-scanner using the two sensors simultaneously using a MISO controller. Both $\mathcal{H}_2$ and $\mathcal{H}_\infty$ controllers are designed to obtain the desired frequency separation in closed loop performance. These controllers are investigated in detail to understand the underlying structure of these controllers and the inherent sensor fusion that takes place. This work enables comparisons with traditional Kalman filtering and $\mathcal{H}_\infty$ filtering problems.

ACKNOWLEDGEMENTS

We would like to acknowledge the entire probe-based technologies and nanofabrication team at IBM-Research Zurich. Special thanks to Haris Pozidis and Evangelos Eleftheriou for their contributions to this work.

REFERENCES

J. C. Doyle, K. Glover an P. P. Khargonekar, and B. A. Francis. State-space solutions to standard H_2 and H_∞ control problems. *IEEE Transactions on Automatic Control*, 34 (8):831–847, August 1989.

A. J. Fleming, A. G. Wills, and S. O. R. Moheimani. Sensor fusion for improved control of piezoelectric tube scanners. *IEEE Transactions on Control Systems Technology*, 16 (6):1265–1276, 2008.

M. G. Forrester, J. Ahner, M. D. Bedillion, C. Bedoya, D. G. Bolten, K. Chang, G. de Gersem, S. Hu, E. C. Johns, M. Nassirou, J. Palmer, A. Roelofs, M. Siegert, S. Tamaru, V. Vaithyanathan, F. Zavaliche, T. Zhao, and Y. Zhao. Charge-based scanning probe readback of nanometer-scale ferroelectric domain patterns at megahertz rates. *Nanotechnology*, 20:225501, 2009.

A. Jo, W. Joo, W. Jin, H. Nam, and J. K. Kim. Ultrahigh-density phase-change data storage without the use of heating. *Nature Nanotechnology*, 4:727–731, 2009.

M. A. Lantz, G. K. Binnig, M. Despont, and U. Drechsler. A micromechanical thermal displacement sensor with nanometer resolution. *Nanotechnology*, 16:1089–1094, May 2005.

M. A. Lantz, H. Rothuizen, U. Drechsler, W. Haeberle, and M. Despont. A vibration resistant nanopositioner for mobile parallel-probe storage applications. *Journal of Microelectromechanical Systems*, 16(1):130–139, February 2007.

I. A. Mahmood, S. O. R. Moheimani, and K. Liu. Tracking control of a nanopositioner using complementary sensors. *IEEE Transactions on Nanotechnology*, 8 (1):55–65, 2009.

A. Pantazi, A. Sebastian, T. Antonakopoulos, P. Bächtold, T. Bonaccio, J. Bonan, G. Cherubini, M. Despont, R. A. DiPietro, U. Drechsler, U. Dürig, B. Gotsmann, W. Häberle, C. Hagleitner, J. L. Hedrick, D. Jubin, A. Knoll, M. A. Lantz, J. Pentarakis, H. Pozidis, R. C. Pratt, H. Rothuizen, R. Stutz, M. Varsamou, D. Wiesmann, and E. Eleftheriou. Probe-based ultra-high density storage technology. *IBM Journal of Research and Development*, 52(4/5):493–511, 2008.

A. Pantazi, A. Sebastian, G. Cherubini, M. Lantz, H. Pozidis, H. Rothuizen, and E. Eleftheriou. Control of MEMS-based scanning-probe data-storage devices. *IEEE Transactions on Control Systems Technology*, 15 (5):824–841, 2007.

A. Pantazi, A. Sebastian, H. Pozidis, and E. Eleftheriou. Two-sensor-based $\mathcal{H}_\infty$ control for nanopositioning in probe storage. In *Proceedings of the IEEE Conference on Decision and Control, Seville, Spain*, pages 1174–1179, December 2005.

H. Pozidis, G. Cherubini, A. Pantazi, A. Sebastian, and E. Eleftheriou. Channel modeling and signal processing for probe storage channels. *IEEE Journal on Selected Areas In Communications*, 28 (2):143–157, February 2010.

S. Salapaka and M. Salapaka. Scanning probe microscopy. *IEEE Control Systems Magazine*, pages 65–83, 2008.

A. Sebastian, A. Pantazi, S. O. R. Moheimani, H. Pozidis, and E. Eleftheriou. Achieving subnanometer precision in a MEMS-based storage device during self-servo write process. *IEEE Transactions on Nanotechnology*, 7 (5): 586–595, 2008a.

A. Sebastian, A. Pantazi, and H. Pozidis. Jitter investigation and performance evaluation of a small-scale probe storage device prototype. In *Proceedings of the IEEE GLOBECOM*, pages 288–293, 2007.

A. Sebastian, A. Pantazi, H. Pozidis, and E. Eleftheriou. Nanopositioning for probe based data storage. *IEEE Control Systems Magazine*, 28 (4):26–35, 2008b.

A. Sebastian and D. Wiesmann. Modeling and experimental identification of silicon microheater dynamics: A systems approach. *Journal of Microelectromechanical Systems*, 17 (4):911–920, August 2008.

K. Zhou, J. C. Doyle, and K. Glover. *Robust and optimal control*. Prentice Hall, 1 edition, 1996.